Journal of Power Sources 219 (2012) 120–125

Contents lists available at SciVerse ScienceDirect

Journal of Power Sources

journal homepage: www.elsevier.com/locate/jpowsour

Short communication

Neutron tomographic investigations of water distributions in polymer electrolyte membrane fuel cell stacks

Henning Markötter [a,*], Ingo Manke [a], Robert Kuhn [b], Tobias Arlt [a], Nikolay Kardjilov [a], Manfred P. Hentschel [c], Andreas Kupsch [c], Axel Lange [c], Christoph Hartnig [b,1], Joachim Scholta [b], John Banhart [a,d]

[a] Helmholtz-Zentrum Berlin (HZB), Germany
[b] Centre for Solar Energy and Hydrogen Research (ZSW), Ulm, Germany
[c] BAM Federal Institute for Materials Research and Testing, Berlin, Germany
[d] Technische Universität Berlin, Germany

HIGHLIGHTS

- Water distribution in fuel cell stacks was analyzed by neutron tomography.
- Changes in the water distribution were observed for 36 h after shut-down.
- Best results were achieved when temperature regulation was switched off.
- Separate analysis of individual cells allows optimization of stack design parameters.

GRAPHICAL ABSTRACT

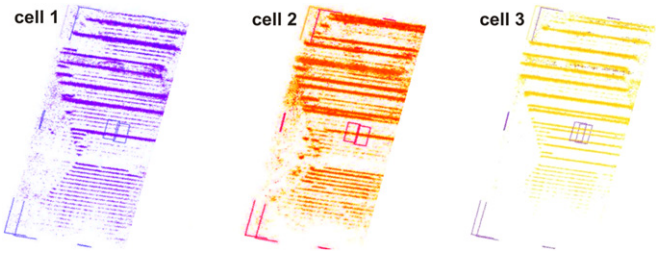

ARTICLE INFO

Article history:
Received 29 March 2012
Received in revised form
22 May 2012
Accepted 14 July 2012
Available online 21 July 2012

Keywords:
Radiography
Tomography
Neutron imaging
Polymer electrolyte membrane fuel cell (PEMFC)
Manifold stack
Water management

ABSTRACT

Neutron tomography was applied to study the 3D water distribution in full polymer electrolyte membrane fuel cell (PEMFC) stacks. The water distribution after switch-off of the fuel cell was analyzed over a period of 36 h. We found a slowly increasing water amount in the fuel cell, but only few changes within a time period of 5 h, which is about the time necessary for neutron tomography. In this way, the requirement for successful tomography was obtained. It is demonstrated how the quasi in-situ tomography technique enables us to study the water content in individual flow field channels of three-fold stacks. Flow field as well as stack design issues are addressed by this visualization method showing weak points due to a non-uniform water distribution that can be identified by means of neutron imaging.

1. Introduction

A substantial part of the recent research on low temperature polymer electrolyte membrane fuel cells (PEMFCs) deals with water management and water transport in fuel cells [1–8]. Only

* Corresponding author.
E-mail address: henning.markoetter@helmholtz-berlin.de (H. Markötter).
[1] Present address: Chemetall, Frankfurt, Germany.

0378-7753/$ – see front matter © 2012 Elsevier B.V. All rights reserved.
http://dx.doi.org/10.1016/j.jpowsour.2012.07.043

a well-balanced humidification ensures a high and stable output power over a long time. Therefore adequate methods for the observation and analysis of water distributions in fuel cells are crucial. In the past years synchrotron X-ray and neutron imaging have been successfully used for this purpose [9–13]. Synchrotron X-ray imaging delivers a high spatial resolution down to 1 μm, which enables the investigation of water transport phenomena inside the pores of the gas diffusion layers (GDLs) in real time [14–19].

Neutron radiography was established as a valuable tool for in-situ investigations of water transport in flow fields on a larger area of interest covering the complete active areas of commercial fuel cells [13,20–27] even as large as 20 × 20 cm^2 [28]. For such measurements typical spatial resolutions range from 25 to 100 μm with typical exposure times between 5 and 60 s. The strong interaction of neutrons with hydrogen is employed to visualize small accumulations of liquid water. Owing to the penetration power of neutrons the metallic end plates and other components appear almost transparent and provide an insight into the internal water distribution of the cell without the necessity of any measurement-related modification to the fuel cells [9].

Radiographic analyses performed in through-plane direction do not allow to separate individual water distributions on the cathode and anode side. In some cases, this drawback could be solved by using different flow field designs on either side [14]. Otherwise, if the anodic and cathodic flow fields bear a large overlap or are operated in the co-flow mode, a distinction of the two sides cannot be easily obtained. From an application point of view fuel cell stacks have to be considered. As the water and thermal management and thus the water distribution differ strongly between single cells and cell stacks and it is not always possible to derive conclusions from one to the other. Therefore, radiography is – in many cases – of limited use for investigations of fuel cell stacks or single cells with overlapping flow field designs. In order to address this limitation several groups have used tomography to analyze the water distribution in fuel cells and fuel cell materials [29–33].

Some years ago a technique was presented that allows for tomographic investigations of fuel cell stacks [34]. For this purpose, gas flow and temperature regulation are temporarily switched off in order to conserve the local water distribution in a fuel cell stack for several hours to fulfill the precondition for 3D imaging by neutron tomography. Here we present new details on the switch-off procedure and investigations on triple fuel cell stacks to prove the unperturbed state of the water distribution.

2. Experimental setup

The investigated triple fuel cell stacks were equipped with multiple serpentine flow fields with 1-mm wide ribs and channels. The individual cells have an electrochemically active area of 100 cm^2. Cooling flow fields were applied to each side of the individual cells with circulating deuterated water, which neutrons can easily transmit. This (heavy) water is tempered to the target temperature to ensure a proper tempering of the cell. GORE® PRIMEA membrane electrode assemblies with a membrane thickness of 19 μm (series 57) and commercial gas diffusion layers (SGL Sigracet® 10BB: thickness 420 μm, with micro porous layer (MPL)) were employed for the fuel cell setup. The fuel cell stack was operated at typical parameter settings: u_C = 40%, u_A = 80%, T = 55 °C, I_0 = 330 mA cm^{-2}, where u_C and u_A are the utilization ratios of the cathodic and anodic gas streams, T the temperature of the thermostat and I the current density. The cathodic gas stream was humidified at a dew point of 25 °C; the anodic gas stream remained unhumidified.

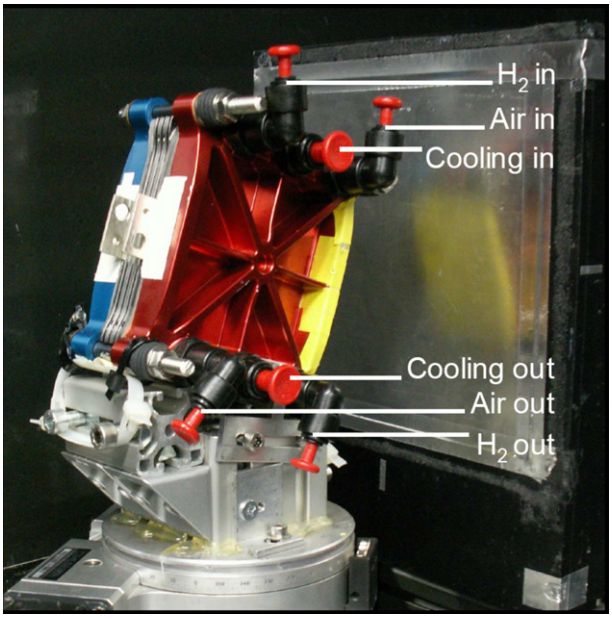

Fig. 1. Triple polymer electrolyte membrane fuel cell stack next to a scintillator screen (right). Gas in- and out-lets were sealed to prevent evaporation.

Neutron tomography was carried out at the CONRAD/V7 (COld Neutron RADiography) facility of the Helmholtz-Zentrum Berlin (research reactor BER II) [35,36]. For each tomography 600 single projections were taken with an exposure time of 30 s per projection. The pixel sizes of the radiographic images were about 110 × 110 μm^2 and the spatial resolution was about 300 μm in the tomogram.

As an example a triple stack positioned in front of the scintillator is shown in Fig. 1. After operation of the triple stack the gas flow was shut off in order to keep the water distribution in the channels at an almost constant level for several hours. The small residual changes of the water distribution were observed by radiographic imaging for different settings.

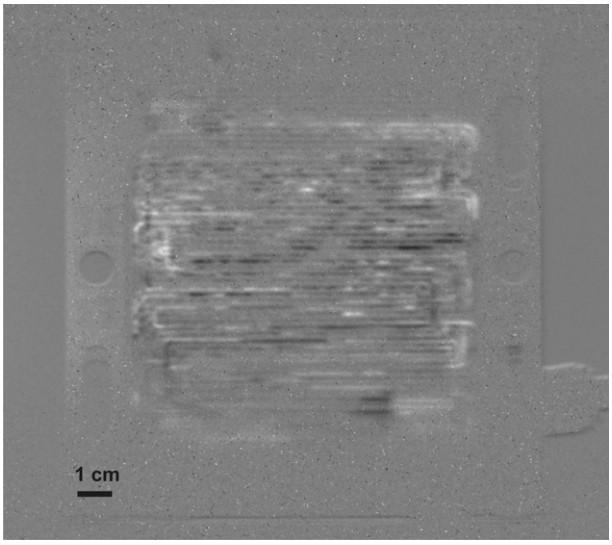

Fig. 2. Changes of water distribution in a fuel cell 3 h after operation has been stopped, but temperature regulation has been continued. White: Additional water; Black: Less water.

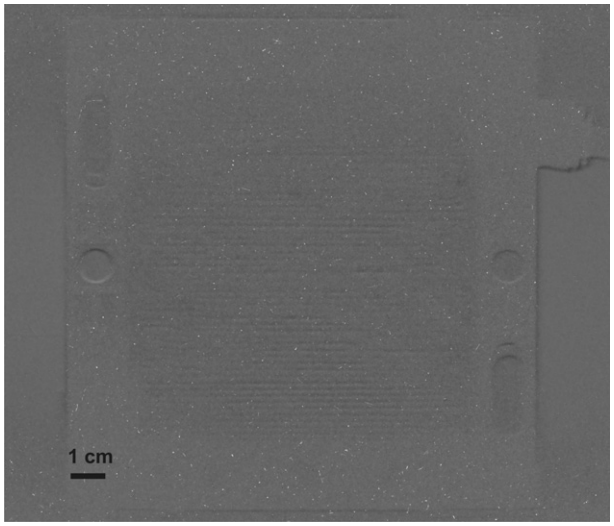

Fig. 3. Changes in the water distribution in a fuel cell 50 min with both, gas supply and temperature regulation have been switched off.

3. Results and discussion

To verify the usability of the experimental procedure described above it is essential to know to which extent the water distribution remains constant throughout the measurement time. In a first approach, the triple fuel cell stack was switched off from stationary operating conditions while the temperature regulation was kept working and also the gas supply tubes were still connected to the cell. The change of the water distribution after about 3 h is displayed in Fig. 2. The neutron radiograph taken directly after the cell had been switched off containing the present water distribution is compared to a radiogram taken 3 h later. The neutron beam attenuation according the Beer–Lambert law causes an exponential decay of the beam intensity:

$$I/I_0 = \exp[-\mu^* d] \quad (1)$$

The inverse calculation delivers the change in thickness of transmitted water.

$$d = \ln(I/I_0)/(-\mu) \quad (2)$$

Where I is the beam intensity of a radiograph of the cell 3 h after it has been switched off, I_0 of the cell directly after it has been switched off, d the thickness of the transmitted water and μ is the absorption coefficient. Black areas mark locations where the water level is reduced and white areas where the water amount has increased. While the overall water amount remained almost constant, the water distribution was strongly altered. Therefore, this switch-off procedure is inadequate since the water distribution has to be kept constant during a tomographic measurement that takes around 5 h.

In the next experiment, in addition to the gas flow the temperature control was also switched off by stopping the pump of the cooling system. After this procedure the temperature of the heavy water in the cooling flow fields and the cell is slowly decreasing to room temperature (25 °C). The image in Fig. 3 shows the changes in water distribution after 50 min. Hardly any changes were found on this short time scale.

Fig. 4 shows the water distribution changes on a longer timescale, describing the situation 9, 18, 27 and 36 h after the cell had been switched off. After 9 h still only a minor increase of the water

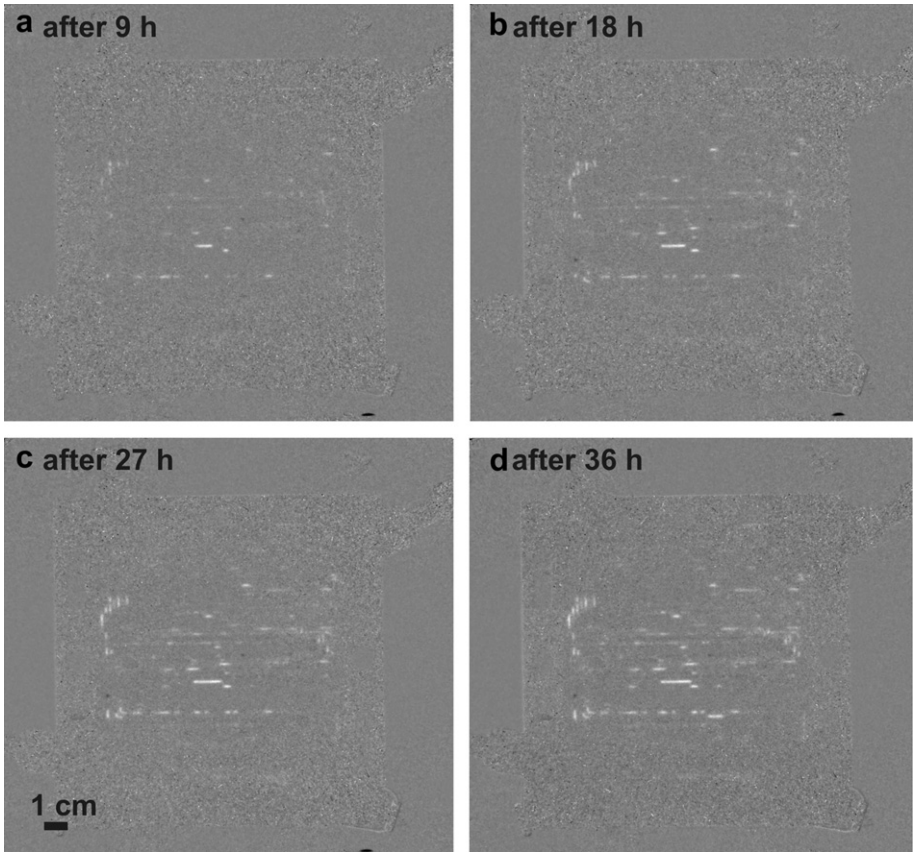

Fig. 4. Changes in the radiographs after 9, 18, 27 and 36 h. Only little change in water distribution occurs, small enough for a proper tomographic reconstruction.

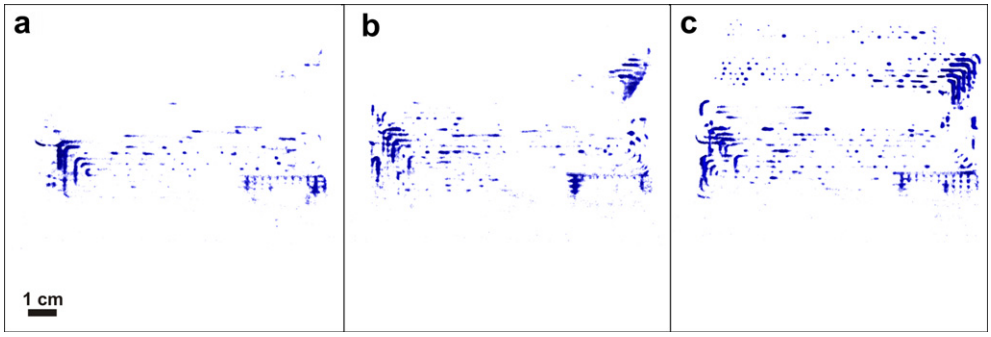

Fig. 5. Water distribution in the individual cells of a three-fold fuel cell stack as measured by quasi in-situ neutron tomography. Cell components are rendered transparent. Most water agglomerates at the turnings of the flow field channels.

distribution at some locations in the channels of the cell can be observed. The additional water amount is about 3% of the overall water content in the cell. Later, the amount of water further increases and finally, after 36 h, an estimated 7–10% of the water content has changed, i.e. mostly additional water (approx. 150 μl) appears due to condensation in the channels. By temperature reduction from 55 °C to about 25 °C the maximum possible amount of gaseous water in 1 m^3 decreases from 104 to about 17 g. That means less than 0.01% of the gas volume in the cell can be water (11 μl) that has condensed due to the temperature drop. This is less than one tenth of the actually observed additional water. Most likely, the additional water in the channels results from agglomeration of homogeneously distributed water in the membrane and GDL, which cannot be identified in the radiographic images. The liquid filled volume is below the detection limit. This water might accumulate after some time in the channels and is detected there as larger droplets reach a critical size. The normalization procedure is not accurate enough to identify homogeneously distributed water in the cell.

From an application point of view it is obvious that the considerable amount of liquid water present in the gas diffusion media has to be removed before the gas supply is stopped and the cell could be subjected to freezing temperatures in real operation conditions. The effect of freezing water on different components has been reported [37,38] as well as the impact on the electrochemically active spots [39]. Our findings underline that transport processes do not stop once the fuel cell has been switched off and both the electrochemical reactions as well as water transport undergo significant changes.

The results presented in Figs. 3 and 4 demonstrate the feasibility of quasi in-situ tomography. Since a tomography experiment takes about 5 h the observed changes in the water distribution do not noticeable disturb tomographic reconstruction. In Figs. 5 and 7 examples of tomographic investigations under the previously determined switch-off conditions are presented.

A three-fold cell stack with serpentine flow fields containing 5 and 11 channels on the anode and cathode, respectively, has been studied. The reconstructed tomogram was used to evaluate the water distribution of the individual cells as well as the individual compartments. Fig. 5 shows the water distributions in the flow field channels for each cell while all other cell components are rendered transparent. In Fig. 5a–c the superimposed anodic and cathodic water distribution is displayed for the three individual cells. The redirection of gas in the turnings of the flow field channels creates favorable conditions for water condensation [40], which is why most water has accumulated in such flow field areas and hence reduce the current density. The link to locally altered current density areas across the electrochemically active area has already been shown by Hartnig et al. [28].

The main advantage of three-dimensional visualization is the differentiation of water present at the anode and cathode flow fields. Even though electrochemical water formation takes place only at the cathode and only the cathodic gas stream is humidified, water is also present in the anodic flow field channels. This can be explained by back-diffusion from the cathode to the anode (see Fig. 6) which is one of the key factors for maintaining a uniform humidification of the active area. This provides the required proton conductivity of the membrane and is common in cells of this type. Water is driven by the concentration gradient through the membrane from the cathode to the anode. This effect counteracts the electro-osmotic drag, which is proportional to the proton density migrating from the anode to the cathode as a consequence of the electrochemical oxidation of hydrogen. Here, the water distribution is influenced by a number of factors with the thickness of the membrane playing an important role. As a comparatively thin membrane (thickness: 19 μm) is employed, sufficient humidification of the anode due to concentration-induced back-diffusion can be easily achieved.

Another three-fold fuel cell stack with a different flow field design has been investigated by quasi in-situ tomography [41,42]. Equipped with a 21-fold meander the flow field represents a compromise between a parallel and a meander flow field with a low number of channels. The parallel flow field results in a low

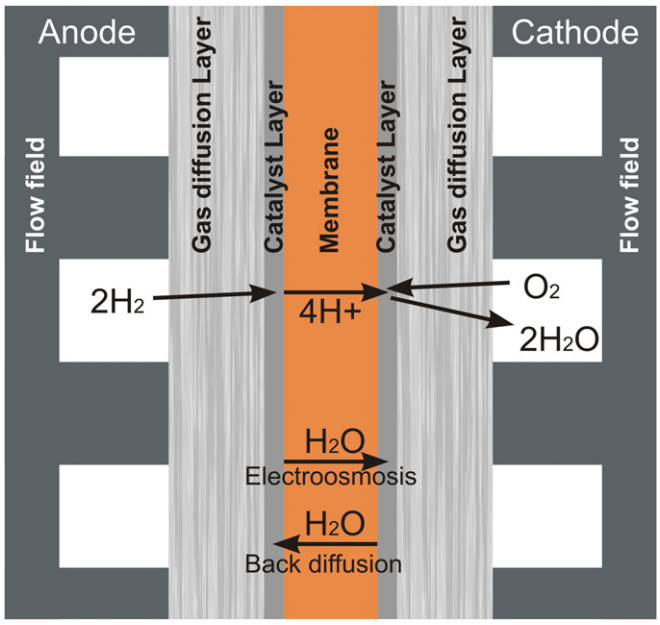

Fig. 6. Reactions taking place in a polymer electrolyte membrane fuel cell.

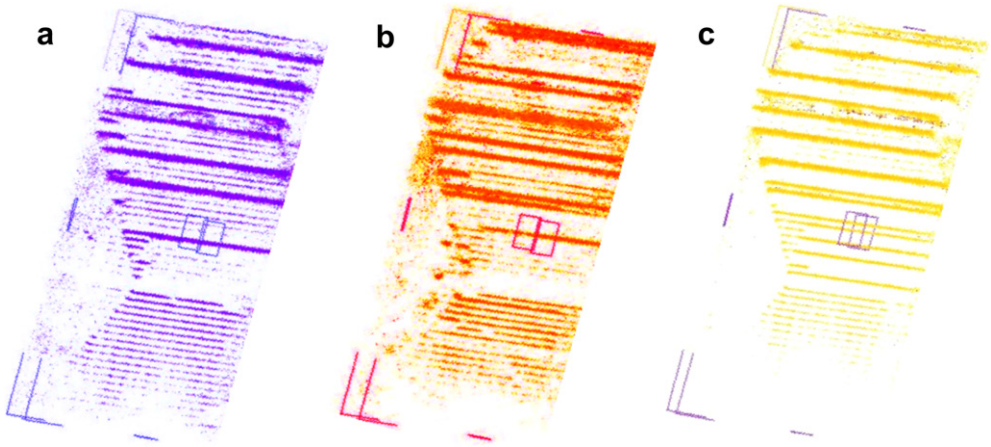

Fig. 7. Separated water distribution for each single cell in a three-fold stack.

gas pressure difference and is therefore prone to liquid water flooding of individual channels. Once a channel is blocked by liquid water the gas stream can easily bypass this channel via water-free alternative 'routes'. In this way flooded channels remain blocked and the problem expands to further channels, thus causing an imbalance of gas supply. The use of a meander flow field with a lower number of channels forces the gas stream to pass the complete flow field or partly stream under the flow field ribs and flow through parts of the GDL. This in turn results in a relatively high pressure drop across the flow field and requires a higher gas pressure which has an impact on the system's efficiency. The use of a 21-fold meander-shaped flow field as shown in Fig. 7 was intended to avoid these disadvantages but still lacks of an inhomogeneous water distribution. While water accumulates in horizontally aligned channel sections, the vertical channel sections stay free of water. An inhomogeneous gas stream might be the reason for this, causing drying parts of the membrane.

Concerning stack design thermal effects might lead to an enhanced condensation of liquid water and cause deviations in the gas flow and pressure of the outermost cells resulting in a decreased performance of these cells. Fig. 7 shows differences in the water amount present in each cell. In triple stacks these effects are not as severe because only limited differences in the amount of water per cell are observed but might play an even more important role in larger stacks. However, neutron tomography is limited due to the attenuation of the beam. With increasing number of cells in a stack the quality of the tomographic reconstruction decreases. Therefore, tomographies of stacks with more than five cells are not yet feasible with the desired quality.

4. Conclusions

Quasi in-situ neutron tomography was used to analyze the water distribution in operating fuel cell stacks in three dimensions. The switch-off procedure was analyzed with different settings. For a tomography that takes about 5 h it is necessary to shut off both the gas flow and the temperature control and for optimal results, in addition, the gas supply tubes should be blocked to prevent water from condensing. For the first time, the water distribution after switch-off of a fuel cell was imaged over a time period of 36 h. However, even after stopping the supply of reactant gases and the temperature control, considerable transport processes take place and some transport of water from the GDL to the flow field channels is observed.

Neutron tomography enables a separate analysis of water accumulations in the individual cells of the stack and allows for a comprehensive study of specific flow field design parameters affecting the water management.

Acknowledgment

The funding of the project RuNPEM (grant numbers 03SF0324B and F) is gratefully acknowledged. The authors also like to thank the German Federal Ministry of Education and Research for the funding of the project with the contract Nos. 03MS607B and D. The authors like to thank A. Hilger (HZB) for beamline support.

References

[1] C.-Y. Wang, Two-phase Flow and Transport, in: W. Vielstich, A. Lamm, H.A. Gasteiger (Eds.), Handbook of Fuel Cells – Fundamentals, Technology and Applications, John Wiley & Sons, Chichester, 2003, pp. 337–347.
[2] A.A. Kulikovsky, T. Wüster, A. Egmen, D. Stolten, J. Electrochem. Soc. 152 (2005) 1290.
[3] S. Litster, D. Sinton, N. Djilali, J. Power Sources 154 (2006) 95–105.
[4] Y. Wang, S. Cho, R. Thiedmann, V. Schmidt, W. Lehnert, X. Feng, Int. J. Heat Mass Transfer 53 (2010) 1128–1138.
[5] C. Ziegler, H.M. Yu, J.O. Schumacher, J. Electrochem. Soc. 152 (2005) 1555–1567.
[6] P. Berg, K. Promislow, J.S. Pierre, J. Stumper, B. Wetton, J. Electrochem. Soc. 151 (2004) 341–353.
[7] U. Pasaogullari, C.-Y. Wang, J. Electrochem. Soc. 152 (2005) 380–390.
[8] C.-Y. Wang, Chem. Rev. 104 (2004) 4727–4766.
[9] J. Banhart, Advanced Tomographic Methods in Materials Research and Engineering, Oxford University Press, Oxford, UK, 2008.
[10] I. Manke, H. Markötter, C. Tötzke, N. Kardjilov, R. Grothaussmann, M. Dawson, et al., Adv. Eng. Mater. 13 (2011) 712–729.
[11] J. Banhart, A. Borbely, K. Dzieciol, F. Garcia-Moreno, I. Manke, N. Kardjilov, et al., Int. J. Mater. Res. 101 (2010) 1069–1079.
[12] P. Boillat, G. Frei, E.H. Lehmann, G.G. Scherer, A. Wokaun, Electrochem. Solid-State Lett. 13 (2010) 25–27.
[13] M.A. Hickner, N.P. Siegel, K.S. Chen, D.S. Hussey, D.L. Jacobson, M. Arif, J. Electrochem. Soc. 155 (2008) 427–434.
[14] I. Manke, C. Hartnig, M. Grünerbel, W. Lehnert, N. Kardjilov, A. Haibel, et al., Appl. Phys. Lett. 90 (2007) 174105.
[15] H. Markötter, I. Manke, P. Krüger, T. Arlt, J. Haussmann, M. Klages, et al., Electrochem. Commun. 13 (2011) 1001–1004.
[16] P.K. Sinha, P. Halleck, C.-Y. Wang, Electrochem. Solid-State Lett. 9 (2006) 344–348.
[17] T. Sasabe, P. Deevanhxay, S. Tsushima, S. Hirai, Electrochem. Commun. 13 (2011) 638–641.
[18] I. Manke, C. Hartnig, N. Kardjilov, H. Riesemeier, J. Goebbels, R. Kuhn, et al., Fuel Cells 10 (2010) 26–34.
[19] R. Thiedmann, C. Hartnig, I. Manke, V. Schmidt, W. Lehnert, J. Electrochem. Soc. 156 (2009) 1339–1347.
[20] M.M. Mench, Q.L. Dong, C.Y. Wang, J. Power Sources 124 (2003) 90–98.
[21] R.J. Bellows, M.Y. Lin, M. Arif, A.K. Thompson, D. Jacobson, J. Electrochem. Soc. 146 (1999) 1099–1103.

[22] R. Satija, D.L. Jacobson, M. Arif, S.A. Werner, J. Power Sources 129 (2004) 238–245.
[23] J. Zhang, D. Kramer, R. Shimoi, Y. Ono, E. Lehmann, A. Wokaun, et al., Electrochim. Acta 51 (2006) 2715–2727.
[24] P. Boillat, D. Kramer, B.C. Seyfang, G. Frei, E. Lehmann, G.G. Scherer, et al., Electrochem. Commun. 10 (2008) 546–550.
[25] A. Schröder, K. Wippermann, J. Mergel, W. Lehnert, D. Stolten, T. Sanders, et al., Electrochem. Commun. 11 (2009) 1606–1609.
[26] A. Schröder, K. Wippermann, W. Lehnert, D. Stolten, T. Sanders, T. Baumhöfer, et al., J. Power Sources 195 (2010) 4765–4771.
[27] N. Kardjilov, I. Manke, A. Hilger, M. Strobl, J. Banhart, Mater. Today 14 (2011) 248–256.
[28] C. Hartnig, I. Manke, N. Kardjilov, A. Hilger, M. Grünerbel, J. Kaczerowski, et al., J. Power Sources 176 (2008) 452–459.
[29] J. Eller, T. Rosen, F. Marone, M. Stampanoni, A. Wokaun, F.N. Büchi, J. Electrochem. Soc. 158 (2011) 963–970.
[30] D.L. Jacobson, D.S. Hussey, E. Baltic, J. Larock, M. Arif, J. Gagliard, et al., Neutron Radiography and Tomography Facilities at NIST to Analyze In-Situ PEM Fuel Cell Performance, Destech Publications, Inc, Lancaster, 2008.
[31] J. Je, J. Kim, M. Kaviany, S.Y. Son, M. Kim, J. Synchrotron Radiat. 18 (2011) 743–746.
[32] J. Kim, J. Je, T. Kim, M. Kaviany, S.Y. Son, M. Kim, Curr. Appl. Phys. 12 (2012) 105–108.
[33] P. Krüger, H. Markötter, J. Haussmann, M. Klages, T. Arlt, J. Banhart, et al., J. Power Sources 196 (2011) 5250–5255.
[34] I. Manke, C. Hartnig, M. Grünerbel, J. Kaczerowski, W. Lehnert, N. Kardjilov, et al., Appl. Phys. Lett. 90 (2007) 184101.
[35] N. Kardjilov, A. Hilger, I. Manke, M. Strobl, M. Dawson, J. Banhart, Nucl. Instrum. Methods Phys. Res. Sect. A: Accel. Spectrom. Detect. Assoc. Equip. 605 (2009) 13–15.
[36] N. Kardjilov, A. Hilger, I. Manke, M. Strobl, M. Dawson, S. Williams, et al., Nucl. Instrum Methods Phys. Res. Sect. A: Accel. Spectrom. Detect. Assoc. Equip. 651 (2011) 47–52.
[37] Y. Wang, P.P. Mukherjee, J. Mishler, R. Mukundan, R.L. Borup, Electrochim. Acta 55 (2010) 2636–2644.
[38] Q.G. Yan, H. Toghiani, Y.W. Lee, K.W. Liang, H. Causey, J. Power Sources 160 (2006) 1242–1250.
[39] Y. Wang, J. Electrochem. Soc. 154 (2007) 1041.
[40] N. Pekula, K. Heller, P.A. Chuang, A. Turhan, M.M. Mench, J.S. Brenizer, et al., Nucl. Instrum. Methods Phys. Res. Sect. A: Accel. Spectrom. Detect. Assoc. Equip. 542 (2005) 134–141.
[41] A. Lange, M.P. Hentschel, A. Kupsch, Computed Tomography Reconstructions by DIRECTT-2D Model Calculations Compared to Filtered Backprojection. Materials Testing-Materials and Components Technology and Application, Carl Hanser Verlag, 2008.
[42] A. Lange, A. Kupsch, M.P. Hentschel, I. Manke, N. Kardjilov, T. Arlt, et al., J. Power Sources 196 (2011) 5293–5298.